SAND2010-3559C

Miniaturized UV Fluorescence Collection Optics Integrated with Ion Trap Chips

Gregory R. Brady*, Shanalyn A. Kemme and A. Robert Ellis
Sandia National Laboratories, PO Box 5800, Albuquerque, NM, USA 87185-1082

ABSTRACT

For practical quantum computing, it will be necessary to detect the fluorescence from many trapped ions using microscale ion trap chips. We describe the design, fabrication and assembly of a set of diffractive optics for coupling this fluorescence into multimode fibers. The design is complicated by the constraints of the ion trap. In addition, the choice of materials available is restricted to those compatible with ultrahigh vacuum. The completed optics-ion trap assembly has successfully been used to trap ions.

Keywords: diffractive optics, ion trap, quantum computing, lens design, optical design, optical alignment

1. INTRODUCTION

Theoretical work over the past decades has shown that quantum computing has great promise for solving problems that are intractable using conventional methods[1],[2]. This has led to much work on trapping single ions so that their quantum states can be manipulated by excitation with light[3]. The signal from these manipulations is read out using the subsequent fluorescence of the ion. The earliest of these experiments used bulky macroscopic ion traps. More recent work has demonstrated a miniaturized, microscopic ion trap on a semiconductor substrate[4],[5], a development which can lead to larger scale integration of many ion traps to implement more complicated computations[6]. However, the primary technique for exciting and reading out the ions will still be optical. Using bulk conventional optics to direct the excitation beam and to collect the resulting fluorescence will be impractical[7].

As an alternative, we will use miniaturized integrated optics and fiber optics, on the same dimensional scale as the ion traps, to route multiple excitation beams and collect the fluorescence from multiple ions. A sketch of the basic arrangement for a single ion in a trap is shown in Figure 1. A single-mode fiber emits light to excite the ion. This light is focused onto the trapped ion using a microlens. When the ion decays from its excited state and fluoresces, the resulting light is collected using a microlens, which couples the light into a multimode fiber. In this work, we have concentrated on fluorescence collection/detection.

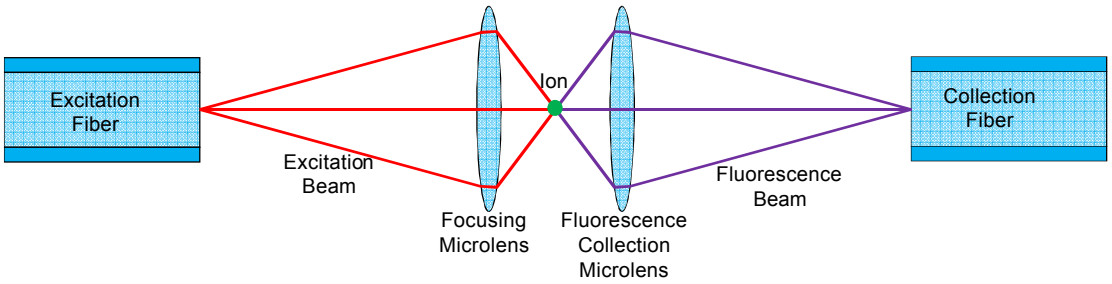

Figure 1. Sketch showing a simplified arrangement for exciting a trapped ion and collecting the resulting fluorescence. The excitation and fluorescence may be temporally and spatially separated.

2. DESIGN

2.1 Design Considerations Particular to Ion Trap Optics

It is only in considering the combined system aspects of the trap chip with integrated optics that an optimum, practical configuration is identified. The arrangement of Figure 1 is conceptually simple, but in reality there are many constraints

* grbrady@sandia.gov; phone 1 505 844-9203; fax 1 505 284-7690; www.sandia.gov

on the optical design because of the necessity of integrating with a functioning ion trap chip, such as that shown in schematic in Figure 2(a). The geometry of the trap chip is tightly coupled to the trapping function and can be altered minimally or not at all for the purpose of integrating optics.

A key consideration is that the emission from a single ion is weak and into 4π steradians, so the collection optics should be of high numerical aperture (NA). Unfortunately there are a number of competing considerations that limit the allowed numerical aperture.

Because the ion is held in the trap using electric fields, static charges on nearby dielectrics, such as our lens aperture, produce a competing electric field near the ion that can perturb the ion trapping field. As a result, the lens should not be particularly close to the ion. The NA is also limited by a choice to place the fluorescence collection optics on the opposite side of the chip from the trapped ion. This was necessary to accommodate the large amount of equipment that needs access to the trap chip from the front side and it is hoped that future sets of integrated optics similar to those presented here will eliminate some of this equipment so that the optics can also placed on the front of the chip. The fluorescence must then be collected through a 100 μm wide slot in the trap electrodes. This slot thus becomes the stop of the system, and its placement is determined entirely by the design of the trap chip. Our optics must be designed to accommodate it. The NA defined by the slot and the desired placement of the ion is 0.37. The lateral dimension of the lens aperture must be kept small to allow for dense integration of the lenses into arrays allowing for many set of optics. This consideration requires that the lens be near the ion, in direct opposition to the desired placement to mitigate charging effects.

In addition, the absolute location of the trapped ion may not be well-controlled, requiring a tolerant design to accommodate these uncertainties. It is anticipated that the lateral position of the ion may vary by as much as ±10 μm, which corresponds to a field angle of as much as 5 degrees. The axial position of the ion from the trap electrodes may also vary significantly, requiring a design robust to focus errors.

The operating wavelength is defined by the wavelength of the fluorescent transition of interest, which is a function of which element is chosen for the trapped ion. This is often in the UV. In this work, we utilized the 397 nm Ca+ transition. The short wavelength limits our choice of materials and complicates the fabrication of the diffractive optics due to the small features necessary.

A further challenge is that the arrangement is used in ultra-high vacuum (10^{-10} to 10^{-11} torr) and may be used at cryogenic temperatures, which places further restrictions on the choice of materials used.

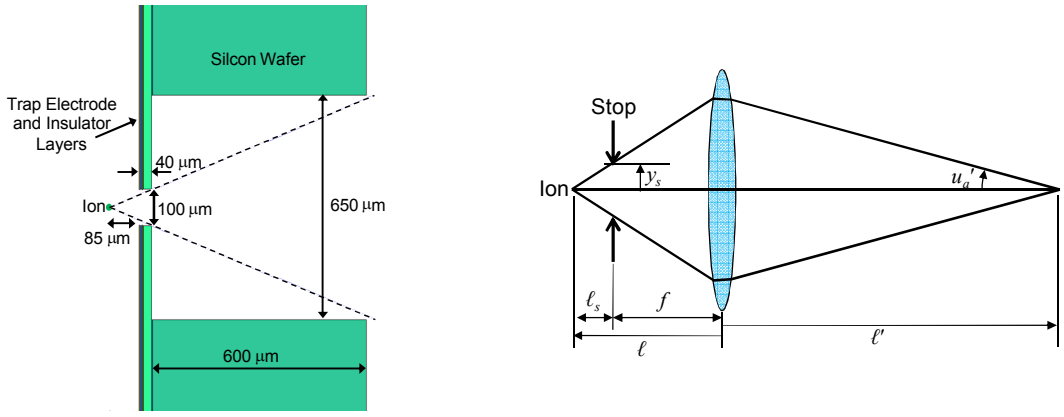

Figure 2. (a) Section through the ion trap chip, showing representative dimensions. Dotted lines indicate the marginal rays from the ion passing through the trap slot, which is the stop for the collection optics. (b) Key parameters for the first order layout.

2.2 First Order Layout

The basic goal of the design is to image the ion onto the end face of the multimode fiber, collecting light from the ion over as large an NA as possible. The resulting image space numerical aperture must be less than the acceptance NA of the fiber to ensure efficient coupling. Thus, we will have a larger object space NA than image space NA, and the

imaging system should have magnification greater than unity. This is an important consideration, since the transverse location of the ion can fluctuate, and the resulting transverse image position will fluctuate to a greater degree because of the magnification. The core size of the fiber must be chosen to accommodate for this. Further, good coupling requires that the image space cone of light falls within the fiber NA for any image position, which we satisfy by ensuring that the imaging is telecentric in image space. This is illustrated in Figure 3. All of these requirements can be satisfied by a few constraints on the first order imaging parameters, defined in Figure 2 (b).

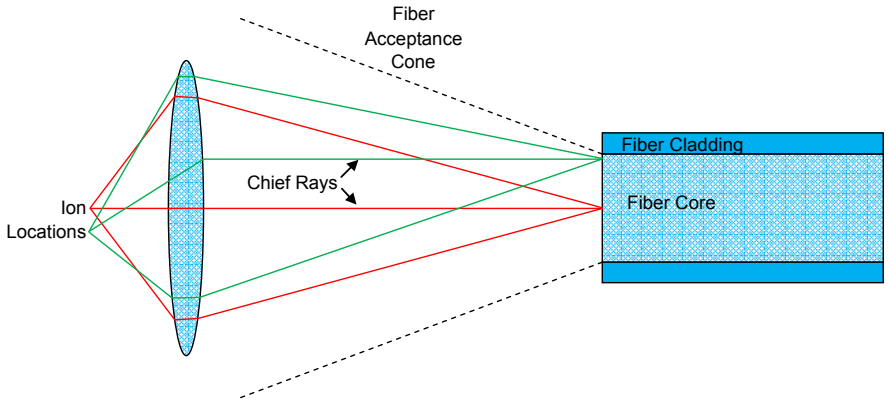

Figure 3. Schematic diagram of optic used to image ions onto fiber core so that the cone of rays forming the image falls on the fiber core and within cone of acceptance of the fiber.

The image space NA, or image space marginal ray angle u_a', is first selected to be smaller than that of the fiber. The object space marginal ray angle $u_a = y_s/\ell_s$ defines the required magnification $m = -u_a/u_a'$. The lens is positioned one focal length away from the stop to ensure telecentricity, so the object distance $\ell = -(\ell_s + f)$. The magnification $m = \ell'/\ell$ is used with the Gaussian imaging equation, $1/f = 1/\ell' - 1/\ell$,to solve for the focal length, $f = -m\ell_s$. This first order thin lens design is used as a starting point for the optimized design below.

The designs were performed assuming that fiber used is Polymicro FVP100110125. The key parameters of this fiber are its core diameter, 100 μm, and its numerical aperture, 0.22. In addition, this fiber has relatively low attenuation at 397 nm. To ensure loose tolerances, we chose the magnification so that the full field point would fall at a radius of 33 μm, well within the core. This results in a magnification of –3 or an image space NA of 0.13, well within the fiber's NA. The dimensions of the trap shown in Figure 2 show that $\ell_s = 85\ \mu\text{m} + 40\ \mu\text{m} = 125\ \mu\text{m}$, so a paraxial thin lens with a focal length of 375 μm would satisfy our design criteria.

2.3 Optimized Diffractive Design

For this first generation of integrated ion trap optics we chose to employ binary diffractive optics largely because they are relatively simple to fabricate. The limited diffraction efficiency means that these elements will not be suitable for final, optimized use, but they allow us to demonstrate the concept and solve many problems before transitioning to a more efficient, and difficult to fabricate, continuous surface relief microoptic.

Two different design forms were considered, both of which are diffractive singlets. Each design was optimized using the Zemax optical design package. The designs were optimized using the default Zemax merit function, with additional terms to keep the chief ray angle small (for telecentricity) and to control the magnification. The first design employs a diffractive only on the optical substrate surface nearest the ion, and the second design employs diffractive elements on both surfaces of the optical substrate. The single-surface design has the benefit of fewer fabrication steps, and possibly less diffractive losses. The two-surface design allows us to use thicker optical substrates and enables better corrected imaging. The two-surface design also allows for optical elements with less power. This results in larger features in the diffractives, which are easier to fabricate and generally have higher diffraction efficiency than a more powerful element. Thus the two-surface design may have efficiency near that of the single surface design. Both designs employ UV grade fused silica, which is compatible with the microfabrication processes used and has good transmission for the design wavelength of 397 nm.

The designs were optimized in Zemax, in particular constraining transverse magnification and chief ray angle to ensure good coupling efficiency. Good designs were obtained by optimizing only the ρ^2 and ρ^4 coefficients in each case. Figure 4 shows a ray trace layout of the two-surface design with the ion placed on axis and with the ion displaced laterally by 10 μm. Geometric fiber coupling analysis predicts 100% coupling efficiency (not including diffraction efficiency and Fresnel reflection losses) at all field angles. The lens is 250 μm in diameter.

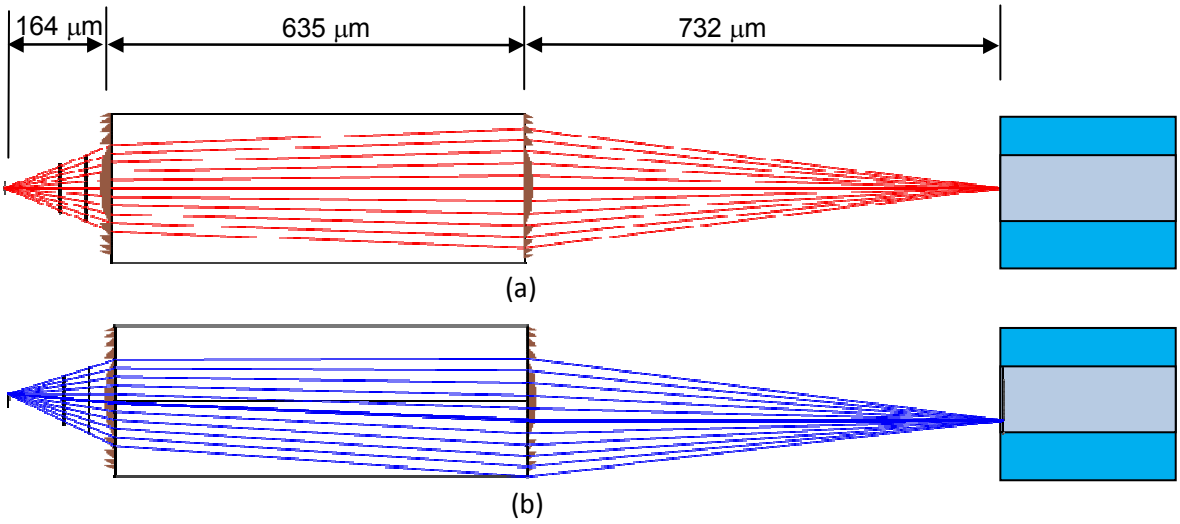

Figure 4. Ray trace depictions of a lens using two diffractive surfaces to couple the light from the ion into a fiber. The first element is f/1.44 and the second is f/1.72. (a) Ion is on-axis. (b) Ion is laterally displaced by 10 μm.

2.4 Nominal performance

The nominal geometrical fiber coupling performance of the two surface optic described above is excellent. All rays traced at each of the different ion positions considered are accepted by the fiber, implying 100% nominal fiber coupling efficiency. Geometric predictions of the image formed at the fiber face are shown in Figure 5. The full scale of these diagrams is the same as the fiber core diameter, so it is clear that all rays fall within the fiber core.

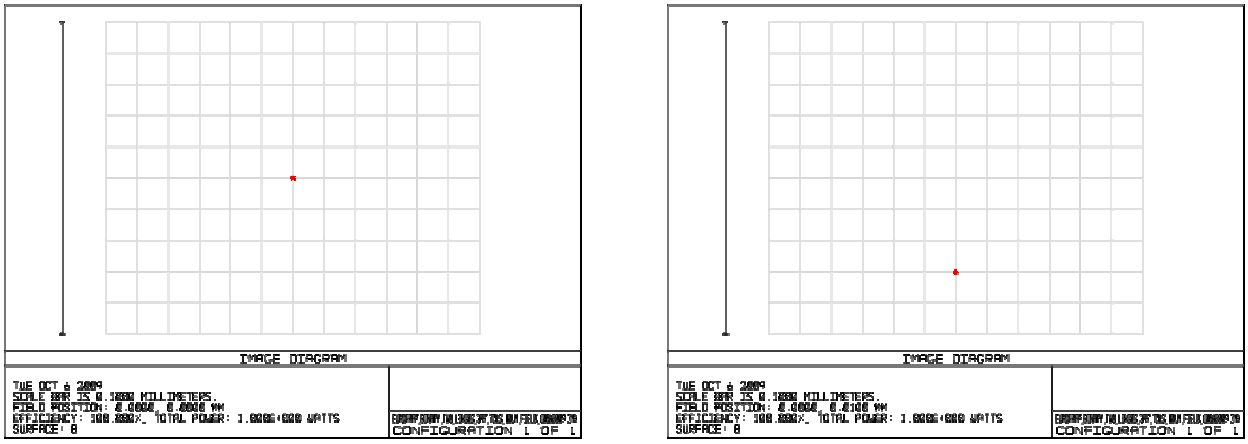

(a) (b)

Figure 5. Geometrical spot diagrams showing image of ion formed at fiber face using two surface design for (a) ion on-axis and (b) ion 10 μm off-axis. The vertical scale here is 100 μm, the same as the diameter of the fiber core, so it is obvious that all rays fall within the core.

3. FABRICATION AND INTEGRATION

3.1 Fabrication

The binary diffractive elements were fabricated using electron beam lithography, as optical lithography is not sufficient to define the small features necessary for optics of this power at this wavelength. The ideal phase profile of the elements were approximated using eight discrete phase levels, requiring three complete lithography cycles. The requires features on the order of 100 nm to be patterned and transferred into the fused silica substrate. This transfer is achieved using reactive ion etching.

Five complete sets of diffractive optics were placed on each 0.5 mm by 1.5 mm optics die on a 250 μm pitch. The lens apertures were chosen to be square to maximize the collection area of each, with the apertures on the ion-facing surface being 140 μm squares and 250 μm squares on the reverse side. A photograph of a number of fabricated optics die appear in Figure 6.

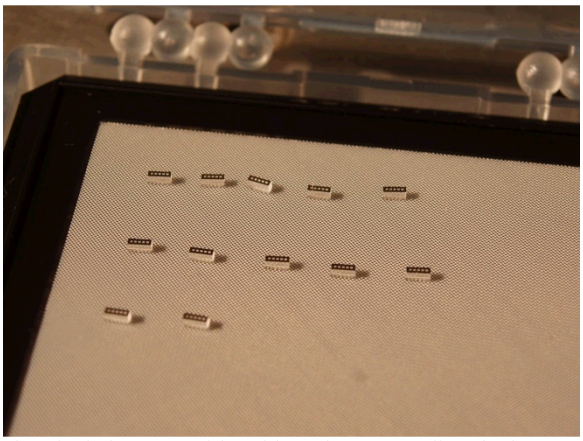

Figure 6. A number of final diced optical elements with gold masks surrounding the lenses. Each die is 0.5 mm x 1.5 mm x 0.635 mm thick.

3.2 Mechanical Integration of Optics and Trap

The approach used to integrate the optics and fibers to the ion trap is illustrated in the drawings of Figures 7 and 8. Firstly, the multimode fibers are held in a commercially available MT ferrule purchased from US Conec, which is composed of a glass filled epoxy material which we qualified for use in vacuum. The as-purchased ferrule includes positions for 12 fibers on a 250 μm pitch, more fibers than needed. In addition, the standard sized ferrule would interfere with the loading procedure for the trap. Our solution to this problem was to cut the ferrule in half, leaving positions for 6 fibers and resulting in a ferrule that blocks only half of the loading slot. The fibers are potted in the ferrule using a vacuum compatible two component epoxy, 3M Scotch-Weld Epoxy Adhesive 2216 B/A, and the end surface of the fibers and ferrule are polished using bound abrasive pads. A machined ceramic (Macor) spacer is the affixed to the end of the ferrule using the same epoxy. The spacer is shaped so as not to block the beam path, and sets the lens to fiber distance as well as the chip to fiber distance. As such the mating surface to the lens is slightly recessed from the chip mating surface. The lens array is affixed to the spacer and the spacer to the chip using the same epoxy. A small drop of conductive adhesive (Johnson Matthey JM7000 Silver Filled Cyanate Ester Die Attach Material) is applied to the gold on the ion-facing surface of the lens array to establish electrical contact with the chip so that the gold will be grounded. Since the area of the bond between the spacer and the chip is relatively small and the ferrule constitutes a relatively large moment arm, a macor piece is added to attach the ferrule to the back of the chip package, taking stress off the spacer-chip bond.

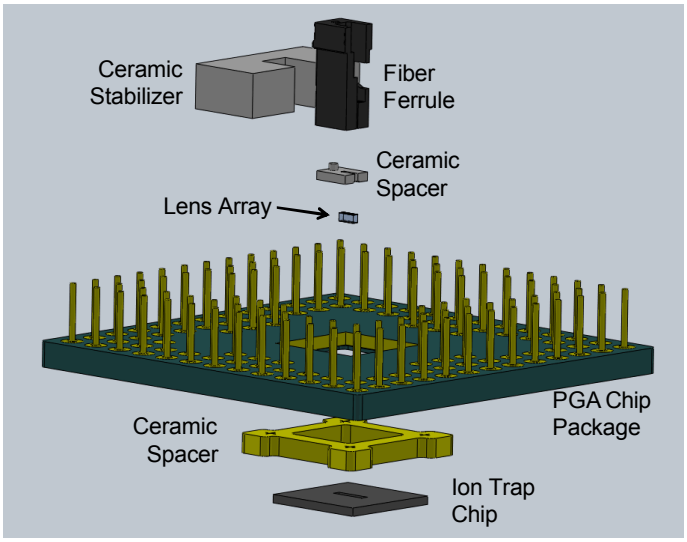

Figure 7. Exploded assembly drawing of the packaged ion trap and the integrated optics.

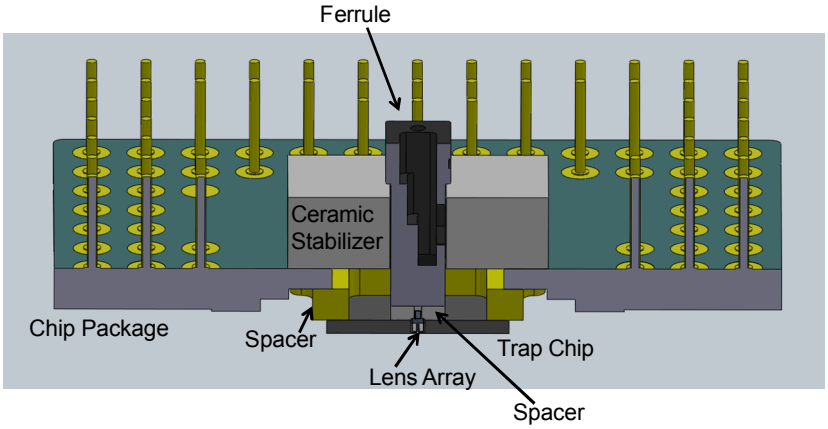

Figure 8. Assembly drawing of the optics integrated with the trap chip.

3.3 Alignment Setup and Techniques

Because of the size and placement of the optics, it was not possible to perform any of the alignments visually or using fiducials. As well, most of the surfaces are not suitable for mechanically registering parts. This led us to employ an active alignment method, where the components are referenced against the position of optical beams simulating an ion, actively optimizing the throughput of the system. These sources were created using an array of 12 single mode fibers, where light has been coupled into two selected fibers. Using two fibers at once is necessary to align for the roll of the arrays about optical axis. Since fiber splitters at this wavelength are not available, the light from the source laser is split using a free space beamsplitter. Each of the two beams passes through a second beamsplitter that is used to gain access to light returning through the source fibers. A sketch of this arrangement is shown in . Coupling the light efficiently to the single mode fibers is challenging because the fiber core for single mode operation at this wavelength is only about 3 μm in diameter.

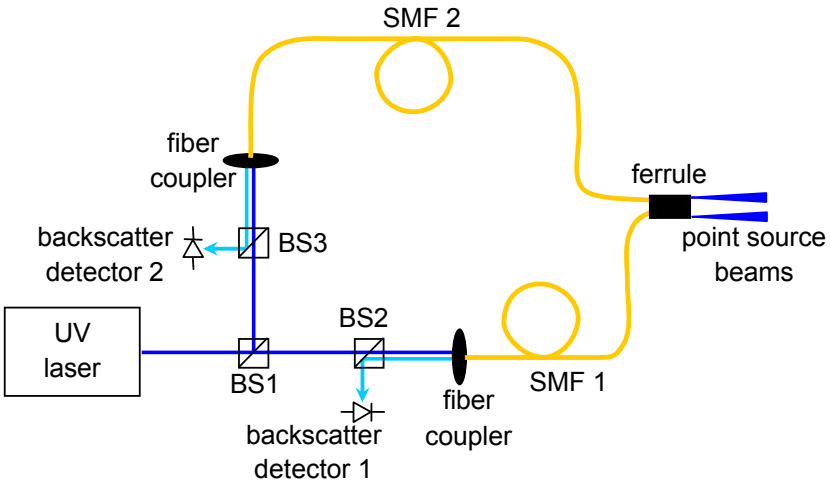

Figure 9. Schematic of setup to produce point source for alignment setup.

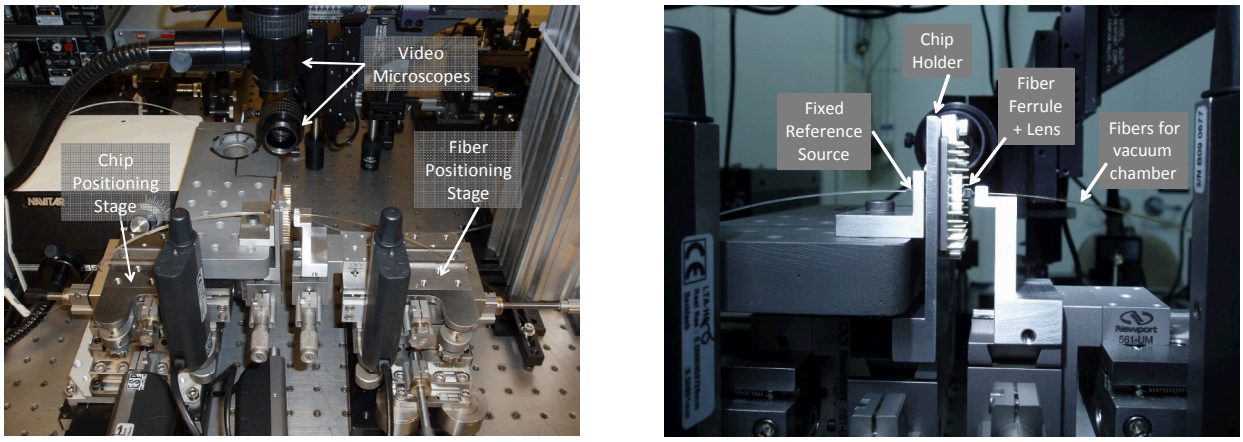

(a) (b)

Figure 10. Photograph of alignment setup, (a) overview showing two six-axis stages for holding the components to be aligned and (b) detail of the fixtures for the fixed reference source, chip and fiber ferrule.

Several experiments were performed to validate steps of the proposed alignment process. With the source fibers in place, we placed a flat mirror directly in front of the sources (held by the stage meant to hold the fiber ferrule of the optics assembly.) The tip and tilt of this mirror was adjusted to reflect light back into the source fibers. When the light coupled back into the fiber is maximized, the tip and tilt is eliminated. This adjustment is necessary to properly align the receiving fibers and the collection optical elements. We were able to successfully detect the light coupled back into the fiber on detectors included with the fiber coupling optics, although in a slightly unexpected fashion. The light reflected off of the mirror unavoidably falls in a spot coincident with the light reflected off of the end face of the input side of the fiber. The light from these two reflections interferes coherently, producing interference fringes that fluctuate dramatically as the alignment is adjusted. Good tip-tilt alignment is ensured by maximizing the modulation of these fringes as the displacement along the optical axis is varied.

We then attempted to couple light directly from the single mode alignment fibers into the multimode fibers by aligning the two sets of fibers so that they are very nearly in contact, known as butt coupling. Tip and tilt of the receiving fibers was adjusted as described above. The roll of the receiving fiber array was adjusted by ensuring that, as the fiber array is moved laterally, the coupled power cuts off at the same point. The lateral position is set by optimizing the power coupled into the receiving fibers when the fibers are far from the source fiber. This sets five degrees of freedom, and the final longitudinal degree is set by bringing the receiving array nearly into contact with the source fibers while visually

observing the movement using a video microscope. Light was efficiently coupled between the two sets of fibers and this proved to be robust to changes in the alignment, as expected with multimode fibers.

3.4 Alignment and Assembly

The first assembly step is to attach the ceramic spacer to the end face of the ferrule. The cut ferrule is shown in its alignment fixture in Figure 11 and the ceramic spacer is shown in Figure 12. This is done by hand using tweezers under a stereo microscope. A small bead epoxy is applied to the ferrule end surface using a scrap of optical fiber. The spacer is then dropped onto the end surface of the fiber and carefully nudged into place visually. This is alignment technique is sufficient, as the lateral position of the spacer is not critical. The epoxy is then cured using a heat gun. The result is shown in Figure 13

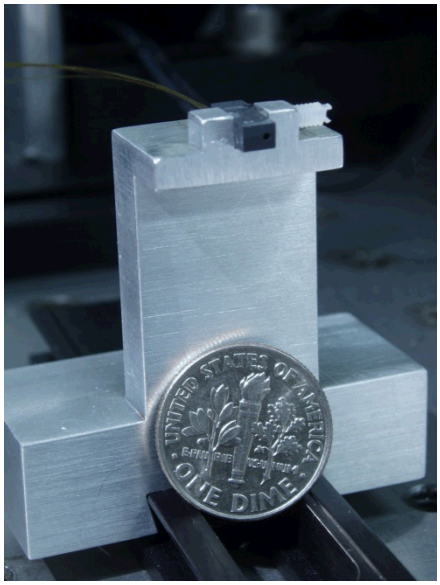

Figure 11. Receiving multimode fibers in ferrule, held in its alignment fixture. A U.S. Dime is shown for scale.

Figure 12. Ceramic spacer to be attached to end of the ferrule.

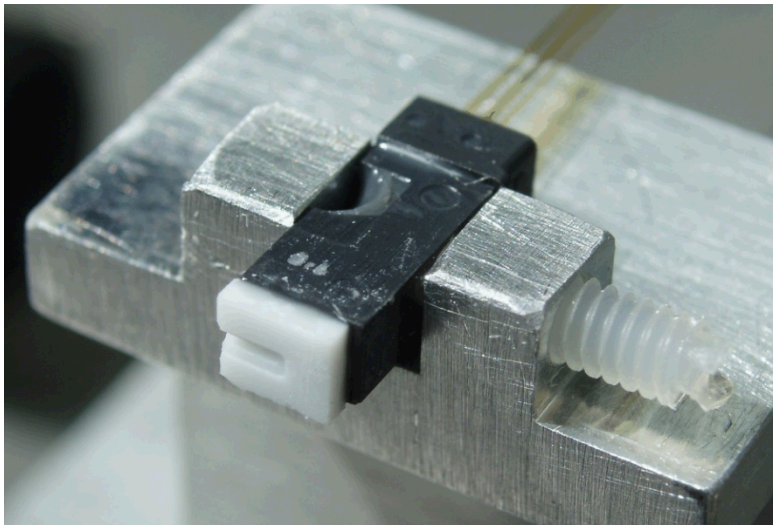

Figure 13. The ferrule with ceramic spacer attached.

The lens array is then attached to the spacer. In order to do this the fiber ferrule with the attached spacer is first aligned to the fixed reference sources. The tip and tilt of the ferrule is aligned visually under the videomicroscopes, roll is eliminated using the technique described in Sec. 3.3, and the lateral position is set by optimizing the coupled power. Focus is not defined at this point, as the longitudinal position of the lens array is set by bringing it in contact with the spacer. The lens array, mounted in a custom fixture under a stereomicroscope, is then placed on the six-axis stage between the source array and the ferrule. This is shown in Figure 14. The tip and tilt of the lens array is set with respect to the ferrule and spacer visually using the videomicroscopes. Roll is eliminated using the technique previously described. The lateral position is set by maximizing the power coupled into the fibers. The axial position is set by bringing the spacer into contact with the lens array, as viewed under the videomicroscopes. The lens array is shown in contact with the spacer but not yet glued in place in Figure 15. Two thin beads of epoxy are then carefully applied by hand using a scrap of fiber along the top bottom edges of the lens array where it contacts the spacer. Excess epoxy typically gets on the face of the spacer at this point and is carefully removed using a dental probe. The epoxy is then cured using a heat gun. The result is shown in Figure 16.

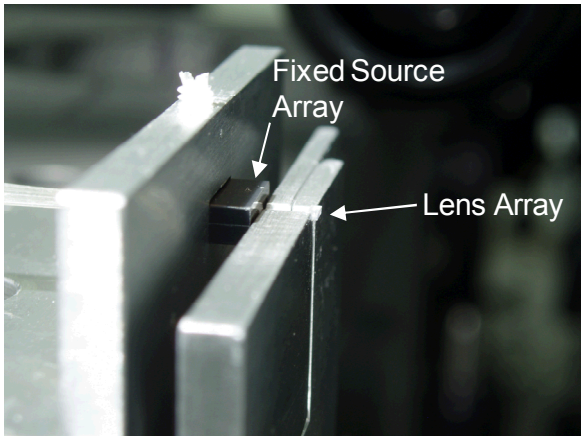

Figure 14. Photograph of fixed reference source array and the lens array in their respective fixtures.

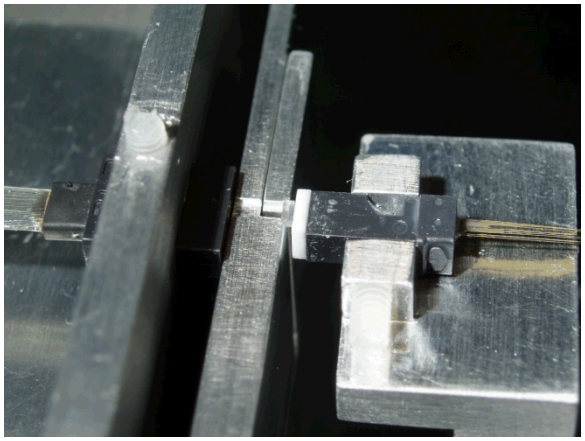

Figure 15. Lens array aligned and in contact with the spacer on the fiber ferrule.

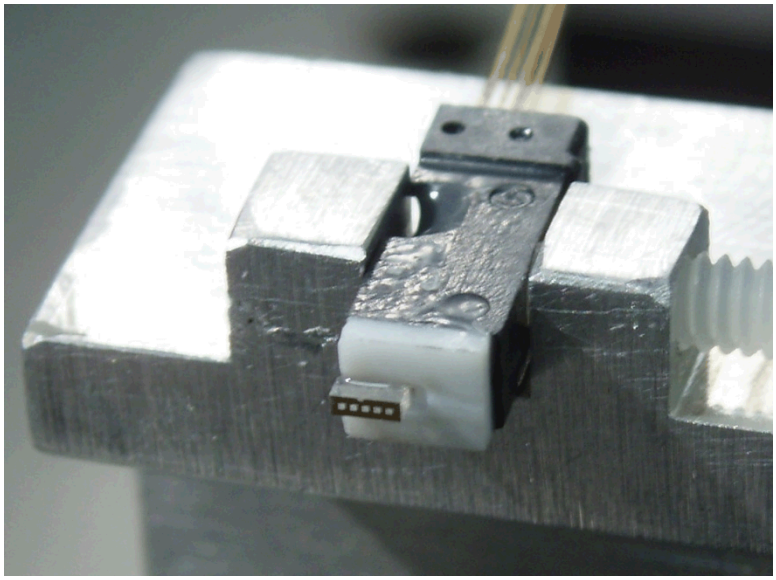

Figure 16. Lens array mounted on the spacer, with the epoxy cured. The gold mask and the five lens apertures are clearly visible.

After the epoxy is cured, the fiber-lens subassembly is realigned to the source array using the same basic techniques as described above with some differences. First, tip/tilt is not set visually, as the highly reflective gold allows us to get significant backreflections into the source fiber. Optimizing these backreflections removes tip and tilt. The longitudinal position of the lens array is set by bringing the array into contact with the source array, and then using a computer controlled actuator on that axis to move the lens back 164 μm to its design position. Once this position is found and noted in the computer, the stage is then moved further back to provide sufficient clearance so that the trap chip can be moved roughly into position and then precisely aligned. The tip and tilt of the trap are set by optimizing the backreflections from the chip's surface. The chip is then moved so that it is very nearly in contact with the source array. The edges of the 100 μm wide slot in the chip are found by noting where the backreflections disappear. Once the position of the source array with respect to these boundaries is established, the chip is moved under computer control so that the reference sources are in a position representative of an ion. Then, the chip is moved back so that the source representing the ion is 85 μm away, axially, from the chip. Epoxy is then applied to the spacer, and a small spot of conductive adhesive is applied to the corner of the lens array contacting the gold, attempting not to obscure any of the lenses. The ferrule-lens array subassembly is brought back into position, so that the spacer is in contact with the back of the chip and the lens array fits inside the slot on the back side of the chip. The epoxy is then cured using a heat gun. A chip with a ferrule and lens array attached is shown in Figure 17.

The final assembly step is to place the mechanical ceramic stabilizer around the ferrule. Epoxy is applied to the mating surfaces of the spacer and it is attached by hand, and the epoxy is cured. This is shown in Figure 18.

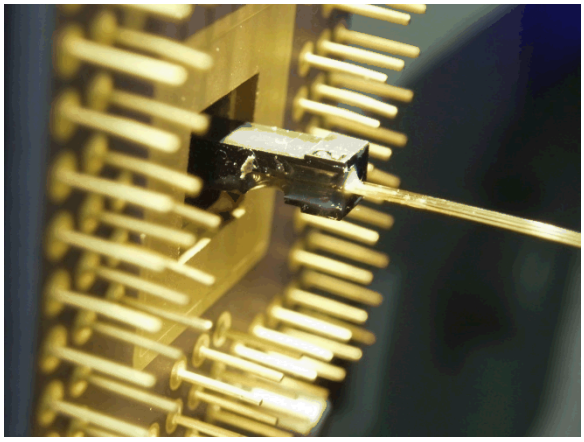

Figure 17. Ferrule-lens assembly attached to the back of the ion trap chip.

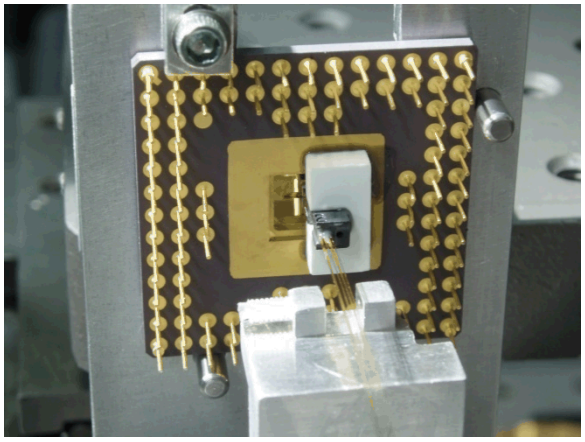

Figure 18. Completed ion trap with optics integrated.

3.5 Installation in Vacuum Chamber and Trapping

The trap chip with attached optics was successfully placed in its vacuum chamber, which was baked out at 150 degrees Celsius and pumped down to a vacuum of 3×10^{-11}, indicating that our materials choices and assembly procedures were indeed suitable for these extremes. A Ca^{+} ion was successfully loaded into the trap and shuttled along the trap, in front of the dielectric of the lens apertures, both of which were feared to problematic operations. The next step in the validation of the trap with integrated optics is to successfully detect photons from the trapped ion at the output end of the multimode fiber. It is anticipated that this will occur within days of the writing of this paper.

4. SUMMARY

We have described the design, fabrication and assembly of the first fiber coupling optics to be integrated with a microscale ion trap chip. We have described a design concept that employs an array of diffractive microlenses to couple fluorescence from a trapped ion into a multimode optical fiber. We identified design constraints particular to the trap, including requirements on the position of the lens, the necessity for compact, high NA optics, and limits on material choices due to the final operating environment. From these requirements we described a first order design procedure and subsequent optimized designs, settling on a two surface diffractive design. An array of this design was successfully fabricated in fused silica, including a gold mask surrounding the lenses to minimize charging effects. We then describe a

strategy and alignment procedure for integrating these optics with the ion trap chip. Finally we reported that the final optic-trap assembly has successfully been used to trap and shuttle ions, a significant achievement. In the very short term we anticipate that we will detect photons from the ion coupled into the fiber.

Future work includes characterization of the coupling efficiency of the optics and the experimental sensitivity to misalignments and ion position. We are considering approaches for fabricating more efficient, continuous surface relief optics to increase the fluorescence collection efficiency. We also plan to fabricate an ion trap whose design is optimized for the integration of optics, so that a larger NA cone of light can be collected. The future optics will also integrated optics for an excitation beam, in addition to the fluorescence collection optics.

Sandia is a multiprogram laboratory operated by Sandia Corporation, a Lockheed Martin Company, for the United States Department of Energy's National Nuclear Security Administration under Contract DE-AC04-94AL85000.

REFERENCES

[1] Richard P. Feynman, "Quantum Mechanical Computers," Found. of Phys. 16(6), 507-531 (1985).
[2] Peter W. Shor, "Algorithms for Quantum Computation: Discrete Logarithms and Factoring," Proc. 35th Ann. Symp. Found. Comp. Sci. (IEEE Comp. Soc., Los Alamitos, CA), 124-134, (1994).
[3] J.I. Cirac and P. Zoller, "Quantum Computation with Cold Trapped Ions," Phys. Rev. Lett. 74(3), 4091-4094 (1995).
[4] D. Stick, W.K. Hensinger, S. Olmschenk, M.J. Madsen, K. Schwab, and C. Monroe, "Ion trap in a semiconductor chip," Nature Physics 2, 36-39 (2006).
[5] D.R. Liebrand et. al., "Demonstration of a scalable, multiplexed ion trap for quantum information processing," Quant. Info. and Comp. 9(11&12), 901-919 (2009).
[6] D. Kielpinksi, C. Monroe, and D.J. Wineland, "Architecture for a large-scale ion-trap quantum computer", Nature 417, 709-711 (2002).
[7] E.W. Streed, B.G. Norton, J.J. Chapman, and D. Kielpinski, "Scalable, efficient ion-photon coupling with phase Fresnel lenses for large-scale quantum computing", Quant. Info. and Comp. 9(3&4), 203-214 (2009).